Research article

Journal of RAMAN SPECTROSCOPY

Received: 5 December 2016 Revised: 3 March 2017 Accepted: 4 March 2017 Published online in Wiley Online Library: 12 April 2017

(wileyonlinelibrary.com) DOI 10.1002/jrs.5147

SERS spectrum of red dyes in the Mapuche belts from the beginning of the XXth century

M. M. Campos-Vallette,[a]* M. J. Rodríguez,[b] M. A. Chapanoff,[b] E. Clavijo,[a] J. S. Gómez-Jeria,[a] A. E. Aliaga,[a] G. P. Jara,[a] F. Celis,[c] C. Paipa[d] and P. Leyton[d]

Red dyes in seven belts (*trariwe*) belonging to the Mapuche culture, dated as beginning of the XXth century and stored in Museo Regional de la Araucanía, Chile, were studied by using ultraviolet-visible, liquid chromatography coupled to mass spectrometry, Raman and Surface Enhanced Raman Scattering spectroscopies. Red dyes were extracted and analysed; the spectral analysis allowed identifying that the principal red dye in five samples is highly consistent with a commercial synthetic aniline, the azopigment PR57. Another monoazopigment, an orange benzimidazolone, was identified in two samples. A molecular model for the PR57/Ag surface interaction supports the idea that the dye mainly exposes to the metal the carboxylate and sulphonate groups; the red azopigment is oriented rather tilted with the two aromatic rings being almost coplanar to the surface. The electrostatic interactions are the main factor of the PR57/Ag layer interaction. Copyright © 2017 John Wiley & Sons, Ltd.

Keywords: SERS; *Trariwe*; Mapuche belts; red dyes; pigments

Introduction

The knowledge of the materials involved in artistic and cultural heritage allows a better understanding of our civilization and an improvement of the restoration and conservation methods. Until recently, the study of works of art remained mainly the concern of research by art historians because the scientific techniques required taking a quantity of samples unacceptable for the integrity of the works. In fact, spectroscopic analyses are the most frequently used methods in the field of cultural heritage.[1,2] Among them, Raman spectrometry is one of the most powerful methods because of its characteristics. The unique properties of this technique involve non-destructive nature, reliability and specificity.[3–5] Thus, Raman spectrometers have become the instruments of choice when analysing archaeological artifacts[6] and pigments or dyes[7] on art works[8] or other materials.[9]

Dyes, the particular interest of the present contribution, together with binders and fillers, provide important information about artists, artistic schools or technological evolution. Nevertheless, the existence of fluorescence in natural dyes and the study of materials present in trace concentrations, two practical and problematic situations, can be surmounted by using the surface enhanced Raman scattering (SERS) technique.[10–21] Recently, Leona *et al.*[12] and Cañamares *et al.*[22] developed new techniques allowing the *in-situ* SERS detection of dyes in textiles. This methodology could be used to detect mordanted colourants; this means to work without any previous hydrolysis of the complex with the mordant and/or without chemical extraction of the dye. The dye interacting with the metal mordant displays SERS effect. A recent study concerned the SERS detection of red organic dyes in Ag-agar gel; it deals with a new method based on the use of a SERS probe made of agar/agar coupled with silver nanoparticles (Ag/agar), for a non-destructive and minimally invasive micro-extraction of dyes from textiles.[23] Highly structured SERS-band intensities were obtained.

This paper reports on the first SERS spectroscopic investigation of red dyes in Mapuche textiles, in particular from multicolour belts or *trariwe*, belonging to the Regional Museum of the Araucanía, Chile. The selected *trariwe* are a fundamental component of the traditional clothing of the Mapuche women. The Mapuche culture is one of the distinct original people mainly settled during the pre-Columbian period in the VI to X Regions of the actual Chilean territory. Mapuche people, from *mapu* land and *che* people, seem to be one of the descendents of the settlers arriving by the Pacific coast route.[24–26] Mapuche textiles have their origins in the pre-Hispanic period possibly having been influenced by the Tiahuanaco, Inca and other northern regional cultures, and later by the Spanish conquerors. The transformations of the Mapuche society, imposed by the Spanish colonization, impacted the textile industry; this activity was influenced by the decrease of large areas of their land, and the appearance of cattle and sheep resources. But the trade did not disappear and, contrary to expectations, began to

* *Correspondence to: M. M. Campos-Vallette, Universidad de Chile, Facultad de Ciencias, Depto. Química, P.O. Box 653 Santiago, Chile. E-mail: facien05@uchile.cl*

a *Universidad de Chile, Facultad de Ciencias, Depto. Química, P.O. Box 653, Santiago, Chile*

b *Museo Regional de la AraucaníaAlemania, 084, Temuco, Chile*

c *Centro de Estudios Avanzados (CEA) y Facultad de Ciencias Naturales y Exactas, Departamento de Química, Universidad de Playa Ancha, Valparaíso, Chile*

d *Instituto de Química, Pontificia Universidad Católica de Valparaíso, Valparaíso, Chile*

Journal of RAMAN SPECTROSCOPY

occupy a strategic place in the indigenous subsistence economy; tissues transactions started to be done through money. Then, this industry produced by women, became an immediate source of income from the late XIXth century and continues today [27]. The Mapuche population generated through history various dyeing techniques mainly to colour their fabrics and wool, with which later made garments, blankets, textiles and numerous things. The colours were completely natural; they were extracted from vegetation, wildlife or minerals found on the land.[28] The yellow colour was extracted from *Piper angustifolium* (*matico*) flowers the orange from flowered *Embothrium coccineum* (*notro*) and *Aristotelia chilensis* (*maqui*) leaves provided the purple tonality. Vegetal red dyes are characteristics of each particular plant; *Relbunium hypocarpium* (*relbun*), for instance, contains purpurine and pseudopurpurine.[29] The natural deep red is hard to find today, probably because of the eventual extinction of the source, *Weinmannia trichosperma* (*tineo*). Here, the identification of the red dyes in Mapuche belts is mainly performed by using Raman and SERS vibrational techniques, and supported with ultraviolet (UV)-visible spectra and liquid chromatography coupled to mass spectrometry (LC–MS) measurements. The dye/metal surface interaction nature is inferred from the SERS bands analysis and the SERS selection rules.[30]

Experimental

Objects and sampling

The Regional Museum of the Araucanía has a collection of 26 textiles registered as girdles or *trariwe* dating from the first half of the 20th century; much of the *trariwe* were collected by *A. Gordon* near Temuco.[31] *Trariwe* are described in various states of preservation or deterioration in the system of administration of the heritage collections of the Chilean DIBAM Museums.[32] We worked with seven belts belonging to the Museo Regional de la Araucanía; samples are listed as 906-2247-2253-2261-2265-2396-3357 (Fig. 1). The analysis of these samples was focused on the red colour, black, white, blue, green and brown colours being also present. Regarding the red colour, threads displaying various tonalities were chosen. Red samples consisted in threads of 2–3 cm, chosen from any of deteriorated horizontal edges.

Ultraviolet-visible measurements

Threads displaying red colour from each sample were chosen for the UV–visible measurements. Each thread was deposited in a glass tube containing 1 ml of ultrapure ethanol. For the UV-visible measurements, 0.9 ml of each solution was dissolved by adding 1.0 ml of ultrapure ethanol. Spectra were scanned between 200 and 800 nm by using 0.5 cm optical-path quartz cells and a Shimadzu model UV-1800 double beam spectrophotometer; the spectral resolution is 2 nm.

Liquid chromatography coupled to mass spectrometry measurements.

The dye solution in ethanol was evaporated to dryness at 30 °C. The obtained solid was characterized through LC–MS by using a procedure similar to that reported by Conneely *et al.*[33] The solid pigment was re-suspended in 5 μl of absolute ethanol and injected into the liquid chromatograph mass spectrometer Shimadzu LC–MS-2020. A column RP-HPLC C18 Kinetec 75 × 2 mm was used along with an isocratic programme water:methanol (1 : 1) for 15 min. For mass spectrometry measurement, spectrum was obtained in negative mode, the electrospray ionization interface was used at 350 °C, 1.5 l/min sweep gas, 15 l/min of nitrogen as drying gas at −5 kV.

Raman and surface enhanced Raman scattering Surface Enhanced Raman Scattering measurements.

The Raman and SERS measurements were performed using a Renishaw micro-Raman RM 1000 spectrometer, equipped with laser lines 514, 633 and 785 nm. The apparatus is coupled to a Leica

Figure 1. Mapuche belts. [Colour figure can be viewed at wileyonlinelibrary.com]

microscope DMLM and a CCD camera electrically cooled. The Raman signal was calibrated to the 520 cm^{-1} line of silicon using a lens of 50× objective. The laser power on the sample is about 0.2 mW. Acquisition time was set between 10 and 20 s per accumulation; the average of accumulations was 10 with spectral resolution of 4 cm^{-1}. The spectra were recorded between 100 and 1800 cm^{-1}. Spectral recording conditions and the choice of the laser line to be used is selected in order to avoid degradation of the sample; in this sense, the 785-nm laser line was used for the SERS and Raman spectral scanning.

Preparation of silver nanoparticles

Silver nanoparticles were prepared by chemical reduction of silver nitrate with hydroxylamine.[34] Briefly, the hydroxylamine hydrochloride-reduced colloid was prepared by adding 10 ml of silver nitrate (10^{-2} M) to a 90 ml of hydroxylamine hydrochloride (10^{-3} M) and sodium hydroxide (10^{-3} M) solution. The AgNPs were obtained at room temperature under rapid stirring conditions. The size distribution of the nanoparticles is in the range 60–150 nm, with the most probable size around 80 nm; the full width at half maximum of the silver colloids is 90 nm.[35] The aqueous solutions utilized for the Ag-NPs formation were prepared by using nanopure water. The colloid shows a milky grey colour, and its extinction spectrum showed a maximum ca. 411 nm (Fig. S1). For the extinction spectra, a diode array spectrophotometer Hewlett Packard 8452 A was used. A control of the purity of the colloidal solution was carried out by measuring the Raman spectrum from aggregates dried over a quartz slide at room temperature; only bands due to νAg-Cl at ca. 236 cm^{-1} were observed.

Sample preparation for the Surface Enhanced Raman Scattering and Raman measurements

Some methodologies employed to extract dyes from tissues involve pyridine or ammonia as solvents.[36–38] Threads of 2–3 cm were deposited in a glass tube with 2 ml of an ethanol/water 25% *v*/v solution during 2 weeks; the whole protected from the temperature and light effects. Aliquots of 50 μl of each solution were deposited on quartz slides until the solvent solution was evaporated at room temperature. This procedure was repeated several times in order to concentrate the colourant by using the total of the original solution. Then, 20 μl of the Ag colloidal solution was added to cover different areas of the dried sample. The whole was left on an aluminium-coated slide at room temperature to get dry. The spectra were scanned after 1 week settle. The SERS spectra were registered on different points of the dried dyes directly on the slide. It was not possible to obtain a Raman spectrum for the dyes directly from the threads of the belts because the intense fluorescence masked the Raman signals. Only in the case of the dye extracted from the sample 2396 that it was possible to register directly its Raman spectrum.

Molecular model, methods and calculations for the metal surface/analyte interaction

A model for the metal surface was built as in our previous studies.[39,40] A face centred-cubic structure with d(Ag-Ag) = 0.408 nm was trimmed to get a planar bilayer composed of 324 Ag atoms. Extended Hückel Theory (EHT) was employed to calculate the wave function of the silver bilayer and the analyte. EHT calculations for the analyte were complemented with DFT calculations at the B3LYP/6-311G(d,p) level. It is known that EHT produces qualitative or semi quantitative descriptions of the molecular orbitals and electronic properties because within the Hartree–Fock–Rüdenberg picture, it is compatible with the nonempirical HF method in Roothaan's form.[41] The Hyperchem[42] and Gaussian 03[43] programs were employed for calculations. Molecular mechanics at the Optimized Potentials for Liquid Simulations level was used to optimize the analyte-Ag geometry, keeping the Ag layer geometry constant. The molecule was initially placed at several different distances and orientations from the centre of the Ag layer. The goal of this simplified molecular system is to try to correlate the enhanced bands in the SERS spectrum with the final analyte position at the Ag surface. This direct interaction occurs when thermal agitation carries out the molecules quite close to the surface with no solvent molecules between them. This situation corresponds to one of the conditions allowing obtaining a SERS spectrum (the other is that the molecule–surface interaction must occur on a hot spot). It is worth to mention that the calculations, their analysis and predictions were made prior to the knowledge of the SERS measurements. This methodology was fruitfully used in our previous SERS works for the interaction of diverse analytes with Ag surfaces.[35,44] The Raman spectrum was calculated within DFT at the B3LYP/6-311G(d,p) level of theory after full geometry optimization with the Gaussian suite of programs.[43]

Results and discussion

Ultraviolet-visible spectra

The UV–visible spectra of the samples in Fig. 2 suggest the coexistence of at least two different red dyes structures displaying maxima in the 500–550 nm range. Kim *et al.*[45] reported a broad absorption band peaked at around 540 nm for the red dye 2-naphthalenecarboxylic acid, 3-hydroxy-4-[(4-methyl-2-sulfophenyl) azo], C.I. 15850,[46] also described as Lithol Rubine B, PR57, see Fig. 3.; this is consistent with the probable existence of this dye in the samples 2265, 2247, 906 and 2396 displaying absorption maxima in the range 540–545 nm, see Fig. 2.

These bands show an asymmetric profile towards the blue. In general, the asymmetry in an UV-vis band is due to the vibrational states of the excited state or sometimes to electronic transitions with different oscillator strength to two different electronic excited states. The coloured intense red samples 2253, 2261 and 3357

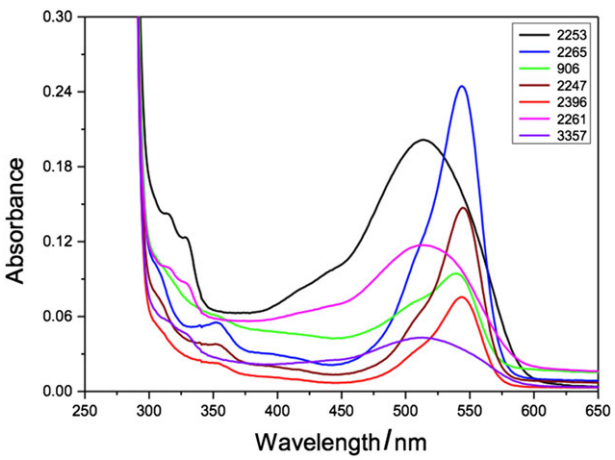

Figure 2. UV-visible absorption spectra of seven ethanolic solutions of red dyed samples. [Colour figure can be viewed at wileyonlinelibrary.com]

Journal of RAMAN SPECTROSCOPY

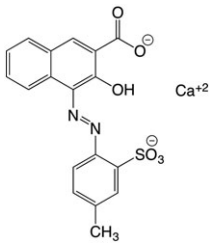

Figure 3. Salt molecular version of the red azopigment PR57 C.I. 15850 [46].

display maxima in the 500–525 nm range; an asymmetric component to the red is observed in the case of the samples 2253 and 2261. Thus, it is expected that the band asymmetry could be related to the coexistence of at least two different structures. The wider bands belong to the samples 3357 and 2253; it is probable that at least two components could coexist in the solution.

Liquid chromatography and mass spectrum

By liquid chromatography, a single peak was found in the solution of dyes extracted from samples 2265, 2247, 906 and 2396 with maxima close to 540 nm at a retention time 0.924 min, indicating a nearly pure compound. Moreover, the mass measured in negative mode, corresponds to the whole molecule (M.M. = 425 amu) without the calcium ion displaying a peak at m/z = 385 amu. Other observed peaks in the defragmentation pattern of the molecule correspond to the stable naphthol and benzyl fragments, consistent with the PR57 azopigment identification. See Fig. 4.

Surface Enhanced Raman Scattering spectra

Only in the case of sample 2396, it was possible to register the Raman spectrum displaying a similar spectral profile of that published for PR57[46] (Fig. 5 and Table 1). This pigment was synthesized at the end of the XIX century.[47] Raman signals were mainly obtained from SERS treatment. The SERS spectrum of the extracted dyes in the solid state, that is the dyes coated by the metal nanostructures, was succeeding, see Fig. 5. The SERS samples maintained the original red colouration. This is highly consistent with the fact that the Raman[46] and SERS spectra profiles for the

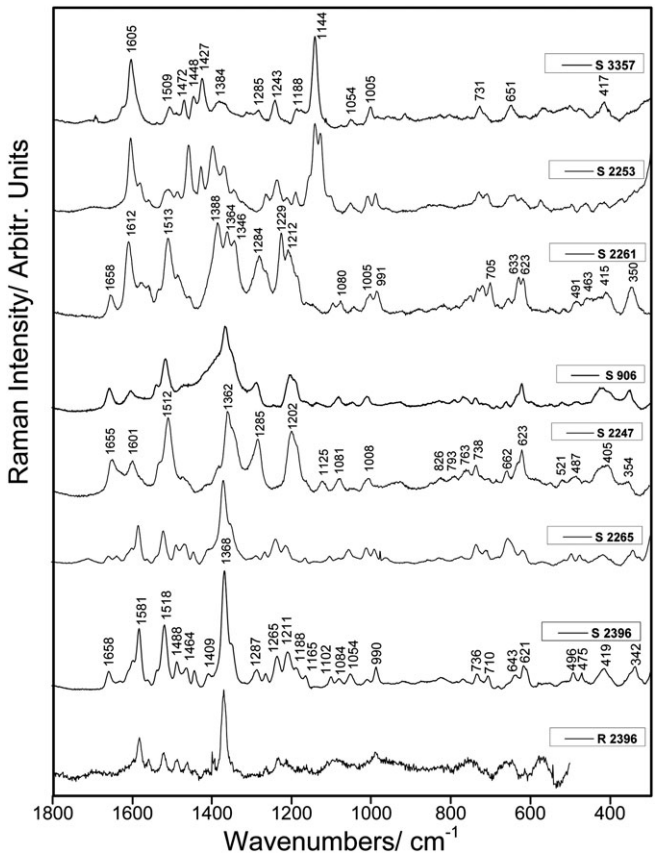

Figure 5. Raman spectrum of sample 2396 (R2396) and SERS spectra of the extracted dyes from samples 2396 (S2396), 2265, 2247, 906, 2261, 2253 and 3357.

extracted red dye in samples, 2247, 2265, 2396 and 906 are not much different (Fig. 5). The spectrum of sample 2261 contains additional information related to some wavenumber shifts and intensity variations. Spectra profile of samples 2253 and 3357 are similar between them but different to those already mentioned. In the group of samples 2247, 2265, 2396 and 906, the spectral differences mainly in the relative intensity and some wave numbers shifts could be related to different orientations of the analytes on the Ag surface, according to the SERS selection rules.[30] In fact, an

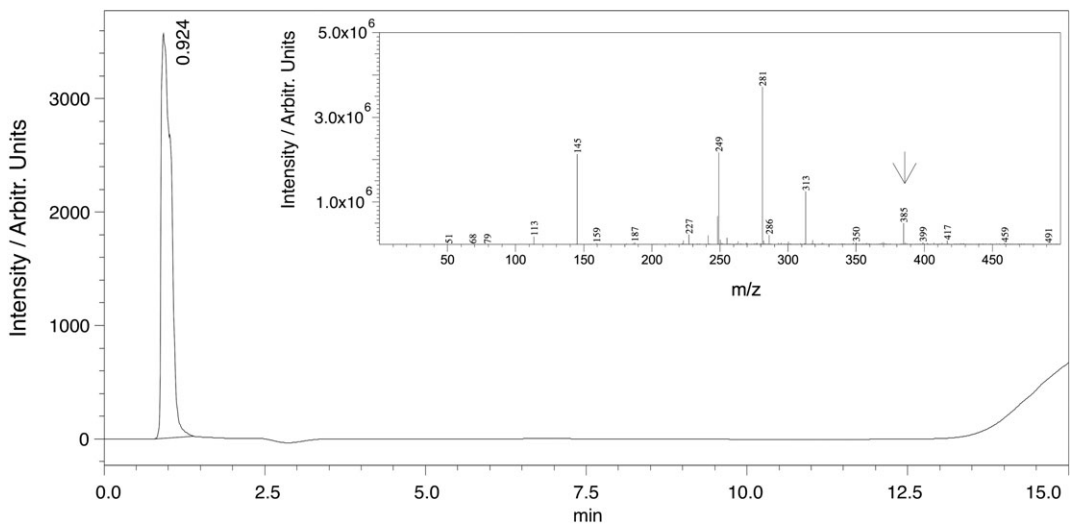

Figure 4. Liquid chromatogram for the red dye dissolved in ethanol and, inserted, defragmentation pattern obtained by mass spectrometry.

Table 1. Experimental and calculated Raman bands (cm^{-1}) of the monoazopigment red dye PR57, C.I. 15850,[46] SERS bands of the red colorant extracted from the Mapuche belt, sample 2396, and the most probable bands assignment

Raman[46]	Raman calc.	SERS	Bands assignment
—	1640	1659 w	νCO, $\nu CC_{arom.}$
1603 s	1616	—	$\nu CC_{arom.}$
—	1584	1581 vw	$\nu CC_{arom.}$
1551 w	1520	—	$\nu CC_{naphth.}$
1491 s	1488	1518 s	$\nu CC_{arom.}$
—	1480	1488 w	Azobenzene ring
—	1448	1464 w	$\delta_{as.}CH_3$
1410 w	1424	1443 w	$\nu N = N$
—	1416	—	νSO_3^-, νCOO^-
1365 vs	1384	1368 vs	νCOO^-, νSO_3^-
1338 w	1344	—	δOH, νCN
1324 w	1336	—	$\nu_{as.}SO_3^-$
1295 w	1280	1288 w	$\nu N = N$
1265 s	1272	1265 w	δCH_3
1229 s	1216	1237 wm 1211 wm	$\nu C\text{-}O$, νSO_3^-
1182 s	1184	—	νSO_3^-,$\nu C\text{-}O$
1129 m	1144	1138 w*	δCH, $\nu C\text{-}O$
—	—	1102 w	ρCH
—	—	1082 vw	ρCH
1038 w	1048	1054 w	ρCH
1020 w	1008	—	ρCH
—	—	990 m	ρCH
965 m	960	—	$\rho CH_{naphth.}$
889 w	912	—	Ring breathing
876 w	864	—	ρCH
820 w	840	—	ρCH
786 w	792	—	Ring def.
765 w	744	—	Ring def.
746 m	736	736 w	ρCH, $\rho CH_{naphth.}$
720 w	704	711 w	$\nu CS_{sulfonate}$
701 w	688	—	$\nu CS_{sulfonate}$
654 w	656	640 vw	Ring def.
597 w	616	621 m	SO_3^- def.
559 w	552	—	Naphth. ring def.
520 m	544	—	Naphth. ring def.
497 m	488	496 w	o.p. Naph.ring def.
467 w	480	475 w	o.p. Naph. ring def.
431 w	424	—	o.p. ring def.
415 w	416	419 wm	Naphth. ring def.
362 m	384	342 m	CCN def.
334 m	320	326 m	τCH_3, τSO_3^-
308 w	288	293 w	τCH_3
261 w	240	—	Naphth. ring def.
202 w	192	—	τSO_3^-
148 m	144	—	τNaphth. ring, τSO_3^-

Abbreviations: ν, stretching, δ, deformation; ρ, out-of-plane deformation; τ, torsion; strong; w, weak; m, medium; d, double; def., deformation; naphth., naphthalene ring, o.p., out-of-plane; arom., aromatic.

* In samples 2247 and 906.

SERS, Surface Enhanced Raman Scattering.

intensity increasing of a band will be verified when the α_{zz} polarizability component of the vibrational mode is parallel to the polarization plane of the electrical field of the incident laser beam.

In the case of samples 2253 and 3357, different orientations could be also proposed for the same molecular system. The SERS spectrum of sample 2253 displays several double bands probably because of the coexistence of conformational species.

The spectral analysis of the SERS spectra was performed on the basis of Raman data on related molecular systems,[48–51] and on previous[46] and our own theoretical Raman data for PR57. The present Raman spectrum of PR57 is shown in Fig. 5. In the case of the samples 906, 2247, 2261 and 2265, the SERS bands analysis was performed from the Raman spectrum of the sample 2396; this spectrum is the most representative in the series. The SERS weak band at 1659 cm^{-1} is attributed to a $\nu CO/\nu CC_{arom.}$ coupled mode. This band is observed with a medium intensity in the case of samples 2247, 906 and 2261, and very weak in the case of sample 2265. This spectral behaviour is interpreted in terms of a different orientation of the corresponding C-OH and CC moieties on the metal surface of the sample 2265 where the corresponding modes are vibrating parallel to the surface. The medium bands at 1581 and 1518 cm^{-1} belong to aromatic νCC vibrations. The band at 1581 cm^{-1} is observed with a weak intensity in the case of the samples 2247 and 906; this is interpreted in terms that an aromatic ring of the dye is probably oriented nearly parallel to the surface. The other aromatic νCC mode at 1518 cm^{-1} slightly modifies its relative strong intensity in the series, which probably indicates that the corresponding ring moiety is tilted to the surface and this inclination is more pronounced in samples 2261 and 2247 where the relative intensity of the CC band is the most intense. The weak bands at 736, 496 and 475 cm^{-1} indicate the presence of a naphthalene moiety; the spectral behaviour by surface effect of these bands ascribed to out of plane ring vibrations is nearly the same in the series of samples. This ring should be preferentially oriented plane parallel to the surface. The band at 1488 cm^{-1} is ascribed to a stretching vibration of the azobenzene ring; this band maintains the relative weak intensity in the series of samples by surface effect, which means that the corresponding ring is not exactly plane parallel to the metal surface. The weak bands at about 1443 and 1287 cm^{-1} are mainly due to the $\nu N = N$ of aromatic azocompounds; the intensity variation of the second band in the series could indicate that this fragment is not parallel to the surface in samples 2261 and 2247 where the relative intensity of the band is medium strong. The strongest band at 1368 cm^{-1} is attributable to a symmetric stretching vibration of the carboxylate group coupled to sulphonate symmetric and asymmetric stretching modes which are expected in this region and close to 1200 cm^{-1} as mainly observed in the spectrum of samples 2247, 906 and 2261. Both bands are not observed in the spectrum of samples 2253 and 3357. The first band maintains the strong relative intensity in the series except in samples 2253 and 3357, and the second is observed relatively weak only in the spectrum of samples 2265 and 2396. This spectral behaviour by surface effect indicates that both the carboxylate and sulphonate groups are oriented towards the metal surface, except in samples 3357 and 2253. The weak band at 1265 cm^{-1} is assigned to a δCH_3. The medium strong band at 1237 cm^{-1} contains information of a carboxylic νC-O mode. The weak band at 1125 cm^{-1} only observed in sample 2247 probably results from coupled δCH and νC-O modes. Out of plane CH deformations, ρCH, are assigned to the bands at 990 and 736 cm^{-1}; the last band is observed with weak intensity in the series, which suggests that the molecular fragment is nearly plane parallel to the surface. This proposition is supported by the similar spectral behaviour of the ρCH band at 1054 cm^{-1}; the spectral assignment is proposed on the basis of the calculated Raman

spectrum data. Weak bands in this spectral region are due to ring deformations. The weak band at 710 cm^{-1} is ascribed to νCS involving the sulphonate group. The medium band at 621 cm^{-1} is probably a deformation of the -SO_2-O- moiety; this band modifies its spectral profile in the series, which support the idea of a different orientation of this vibrating moiety of the molecules on the metal surface. Bands below 500 cm^{-1} are ascribed to ring deformations in particular the weak bands in the 470–500 cm^{-1} region which are attributable to out of plane ring deformations. These bands modify their intensity and wavenumber in the series suggesting that these ring vibrations belong to a moiety rather tilted to the surface. The weak band at 342 cm^{-1} involves the CCN molecular fragment. Weak and very weak bands observed only in the Raman spectrum[46] at 1338, 889, 720, 559 and 431 cm^{-1} were also assigned. The first band is a δOH/νCN coupled vibration, and the second is a ring breathing mode; the band at 720 cm^{-1} is a νCS of the sulphonate group while the last two bands are ascribed to out of plane ring deformations. On this basis, it is proposed that samples are not organized with an identical orientation on the surface; the orientation seems to be different in each sample. Table 1 contains the present and published[46] Raman bands, and the calculated Raman wavenumbers of PR57, and the SERS data for sample 2396 along with the most probable bands assignment.

The SERS spectrum signals must correspond to those species displaying the optimal organization and orientation on the metal surface; this is consistent with the fact that two different coexisting molecules could not be simultaneously identified. The SERS spectra of the samples 2253 and 3357 in Fig. 5, resulted very similar but different to that of the samples 906, 2247, 2261, 2265 and 2396. The SERS wavenumbers of samples 2253 and 3357 are quite close to the Raman data published[46,50] for the monoazopigment PO36, benzimidazolone (2-((4-chloro-2-nitrophenyl)azo)-N-(2,3-dihydro-2-oxo-1H-benzimidazol-5-yl)-3-oxo-butanamide, $C_{17}H_{13}ClN_6O_5$), Fig. 6, which is highly consistent with the present SERS results; this compound was patented in 1963.[52]

It is not excluded that this compound or another related benzimidazolone were used in restored areas as it is possible to observe in the *trariwe* 3357, Fig. 1. The following spectral assignment based on published data[48,49,51] and those reported by Colombini *et al.*[50] in PO36 and by Suwaiyan *et al.*[53] in benzimidazole and Krishnakumar *et al.*[54] in the fragment 2-hydroxybenzimidazole, supports the present proposition. The most intense SERS bands of the sample 3357 at 1605 and 1144 cm^{-1} are attributed to νCO/$νCC_{arom.}$ and to the breathing mode of the 5-membered ring, respectively. The weak bands at 1509 and 1472 cm^{-1} are assigned to the aryl-NO_2 fragment. The band at 1472 cm^{-1} is a CH_3 deformation. The weak band at 1448 cm^{-1} is probably the νNN mode, while the medium bands at 1427 and 1243 cm^{-1} are ring stretching and CH in plane modes, respectively. The broad and weak band at about 1390 cm^{-1} is a symmetric $νNO_2$ mode. The weak bands at 1054 and 1004 cm^{-1}, are ascribed to aryl-Cl vibrations; bands at 830, 805 and 731 cm^{-1} are mainly due to ring CH out of plane deformations. The medium weak band at 917 cm^{-1} could correspond to a ring breathing mode. The broad and weak bands at 651, 572, 483 and 417 cm^{-1} are due to ring in and out-of-plane deformations.

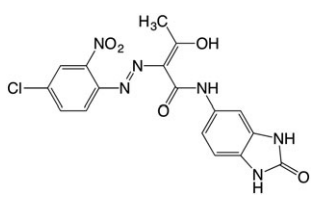

Figure 6. Chemical structure of PO36, benzimidazolone pigment.

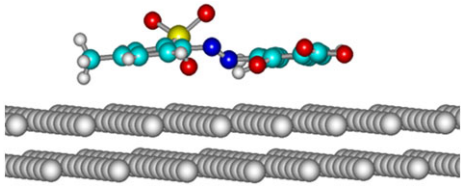

Figure 7. Molecular model for the PR57/Ag surface interaction. [Colour figure can be viewed at wileyonlinelibrary.com]

Calculations on the PR57/Ag interaction

In the final interaction geometry, Fig. 7, the dye is positioned at the centre of the metallic layer; the two aromatic rings being almost coplanar to the surface. Considering that the frontier MOs of the pigment do not overlap with the frontier MOs of the Ag bilayer, a charge transfer is ruled out.[44,55] Therefore, we may conclude that electrostatic interactions are the main factor of the PR57/Ag layer interaction. The shortest distances from the dye to the Ag layer are O from COO^-: 0.32 to 0.34 nm, O from SO_3^-, are in the range 0.30–0.33 nm, O from OH: 0.30 nm, H from OH: 0.25 nm, and H from methyl are in the range 0.26–0.30 nm. The N attached to the naphthyl ring is at 0.30 nm to the closest Ag atom. If the dye molecule is oriented as in Fig. 7, on a hot spot and the laser line is perpendicular to the surface, then bands of the carboxylate group should be enhanced which is in good agreement with the SERS experimental result. This is the case for the strong band at 1368 cm^{-1} and the medium bands around 1230 cm^{-1}; this situation is similar for the medium strong and medium bands of the sulphonate group at about 1200 and 620 cm^{-1}, respectively. Because the model also predicts that one of the aromatic ring fragments is close to the surface, then, the corresponding Raman signals should be influenced by surface effect, which is in agreement with the SERS data for one of the aromatic νCC vibrations displaying a medium strong band at 1518 cm^{-1}. No SERS band ascribed to an eventual Ag-O interaction was identified, which is supported by the calculations predicting the absence of a charge transfer. This is consistent with the fact that the experimental Raman and SERS spectral profiles are not much different; this also explains the similar red colour tonality displayed by the Ag colloidal coated and uncoated samples. Finally, the main contribution to the Raman enhancement, in the case of the PR57/Ag interaction is the electromagnetic mechanism.[56]

Conclusions

The present set of results concerning some Mapuche belts dating beginning of the XX century is consistent with the use of the synthetic aniline monoazopigment PR57 C.I. 15850, the red dye, and with another monoazopigment probably PO36 C.I. 11780 the orange benzimidazolone dye. The UV-visible spectra of the samples suggest the coexistence of at least two different red dyes structures. The LC–MS results support the use of the PR57 red dye, BON lake. The SERS spectral identification of the PR57 dye was based on the present experimental and published

Raman spectra, and the calculated one. The SERS spectrum of samples 2253 and 3357 are dominated by the orange dye, benzimidazolone. It is generally expected that the SERS spectrum signals must correspond to that species displaying the optimal organization and orientation on the metal surface. This is consistent with the fact that at least two coexisting different dyes were not simultaneously identified. Similar SERS spectra profiles were obtained for the red dye extracted from the threads samples; those spectra display mainly intensity differences, which are associated to different orientations of the dye on the metal surface. A molecular model for the PR57/Ag surface interaction allowed confirm that the PR57 dye mainly exposes to the metal the carboxylate and sulphonate groups; the azopigment is oriented rather tilted with the an aromatic ring being almost coplanar to the surface. The electrostatic interactions are the main factor of the PR57/Ag layer interaction. On this basis, and on the fact that the Raman spectrum of benzimidazolone pigment PO36 is not much different from the SERS one, indicates that the metal surface PO36 pigment interaction is also mainly due to electrostatic forces. The identification of the orange dye strongly suggests a rather recent intervention on the samples 3357 and 2253. Finally, we are investigating the origin of the blue and green colours in the same belts in the hypothesis that they could also contain commercial synthetic dyes. The identification of the present complex organic modern red dyes in the analysed *trariwe* should be a health signal mainly to those people dying the tissues.

Acknowledgments

Authors acknowledge projects 1140524 and 3140492 from Fondecyt for financial support. MECESUP UCV-0801 is also acknowledged. FC acknowledge project 3150222 from Fondecyt.

References

[1] P. Baraldi, A. Tinti, *J. Raman Spectrosc.* **2008**, *39*, 963.
[2] P. Vandenabeele, H. G. M. Edwards, L. Moens, *Chem. Rev.* **2007**, *107*, 675.
[3] N. Q. Liem, G. Sagon, V. X. Quang, H. v. Tan, P. Colomban, *J. Raman Spectrosc.* **2000**, *31*, 933.
[4] P. Colomban, F. Treppoz, *J. Raman Spectrosc.* **2001**, *32*, 93.
[5] N. Boucherit, A. Hugot-Le Goff, S. Joiret, *Corros. Sci.* **1991**, *32*, 497.
[6] L. Burgio, R. J. H. Clark, R. R. Hark, *PNAS.* **2010**, *107*, 5726.
[7] P. Vandenabeele, L. Moens, H. G. M. Edwards, R. Dams, *J. Raman Spectrosc.* **2009**, *73*, 505.
[8] Cl. Coupry, *Analusis* **2000**, *28*, 39.
[9] I. Geiman, M. Leona, J. R. Lombardi, *J. Forensic Sci.* **2009**, *54*, 947.
[10] M. Cañamares, J. V. Garcia-Ramos, C. Domingo, S. Sanchez-Cortes, *J. Raman Spectrosc.* **2004**, *35*, 921.
[11] K. Chen, M. Leona, K. Vo-Dinh, F. Yan, M. B. Wabuyele, T. Vo-Dinh, *J. Raman Spectrosc.* **2006**, *37*, 520.
[12] M. Leona, J. Stenger, E. Ferloni, *J. Raman Spectrosc.* **2006**, *37*, 981.
[13] A. V. Whitney, R. P. van Duyne, F. Casadio, *J. Raman Spectrosc.* **2006**, *37*, 993.
[14] M. Leona, J. R. Lombardi, *J. Raman Spectrosc.* **2007**, *38*, 853.
[15] A. V. Whitney, F. Casadio, R. P. van Duyne, *Appl. Spectrosc.* **2007**, *61*, 994.
[16] S. Bruni, V. Guglielmi, F. Pozzi, *J. Raman Spectrosc.* **2010**, *41*, 175.
[17] F. Casadio, M. Leona, J. R. Lombardi, R. van Duyne, *Acc. Chem. Res.* **2010**, *43*, 782.
[18] Z. Jurasekova, E. del Puerto, G. Bruno, J. V. García-Ramos, S. Sanchez-Cortes, C. Domingo, *J. Raman Spectrosc.* **2010**, *41*, 1455.
[19] F. Pozzi, J. R. Lombardi, M. Leona, *Heritage Science* **2013**, *1*, 1.
[20] F. Pozzi, J. R. Lombardi, S. Bruni, M. Leona, *Anal. Chem.* **2012**, *84*, 3751.
[21] C. L. Brosseau, F. Casadio, R. P. van Duyne, *J. Raman Spectrosc.* **2011**, *42*, 1305.
[22] M. V. Cañamares, J. V. García-Ramos, J. D. Gomez-Varga, C. Domingo, S. Sanchez-Cortes, *Langmuir* **2007**, *23*, 5210.
[23] C. Lofrumento, M. Ricci, E. Platania, M. Becucci, E. Castellucci, *J. Raman Spectrosc.* **2013**, *44*, 47.
[24] A. Sala, D. Corach, *Mol. Biol. Rep.* **2014**, *41*, 1533.
[25] D. Rey, C. Parga-Lozano, J. Moscoso, C. Areces, M. Enríquez-de-Salamanca, M. Fernández-Honrado, S. Abd-El-Fatah-Khalil, J. Alonso-Rubio, A. Arnaiz-Villena, *Mol. Biol. Rep.* **2013**, *40*, 4257.
[26] M. de Saint Pierre, C. M. Bravi, J. M. B. Motti, N. Fuku, M. Tanaka, E. Llop, S. L. Bonatto, M. Moraga, *PLoS One* **2012**, *7*, e43486.
[27] A. Willson, in *Textilería Mapuche* (Ed: E. M. y. Cultura), EM, Santiago, Chile, **1993**.
[28] S. H. Chacana, in La mujer del color, usos y significados de los tintes del trariwe o faja femenina, of the Regional Museum of the Araucanía collection. FAIP project, Chile, **2013**.
[29] H. Schweppe, J. Winter, in *Madder and Alizarin* (Ed: E. West FitzHugh), Artists Pigments, vol. *3* , Oxford University Press, Oxford, **1997**.
[30] M. Moskovits, *Rev. Mod. Phys.* **1985**, *57*, 783.
[31] S. H. Chacana, in Diferenciadores de la textualidad y etnoestética femenina contenida en la colección de trariwe del Museo Regional de la Araucanía. Report project Heritage Research Fund DIBAM, Chile, **2012**.
[32] System of administration of the heritage collections of the Dirección de Bibliotecas, Archivos y Museos (DIBAM) de Chile, www.surdoc.cl
[33] A. Conneely, S. McClean, W. F. Smyth, G. McMullan, *Rapid Commun. Mass Spectrom.* **2001**, *15*, 2076.
[34] N. Leopold, B. J. Lendl, *J. Phys. Chem. B* **2003**, *107*, 5723.
[35] M. A. Herrera, G. P. Jara, A. E. Aliaga, J. S. Gómez, E. Clavijo, C. Garrido, T. Aguayo, M. M. Campos-Vallette, *Spectrochim. Acta A* **2014**, *133*, 591.
[36] J. Orska-Gawrys, I. Surowiec, J. Kehl, H. Rejniak, K. Urbaniak-Walczak, M. Trojanowicz, *J. Chromatogr. A* **2003**, *989*, 239.
[37] A. A. Tuinman, L. A. Lewis, S. A. Lewis, *Anal. Chem.* **2003**, *75*, 2753.
[38] A. R. Stefan, C. R. Dockery, A. A. Nieuwland, S. N. Roberson, B. M. Baguley, J. E. Hendrix, S. L. Morgan, *Anal. Bioanal. Chem.* **2009**, *394*, 2077.
[39] P. Leyton, J. S. Gómez-Jeria, S. Sanchez-Cortes, C. Domingo, M. Campos-Vallette, *J. Phys. Chem. B* **2006**, *110*, 6470.
[40] A. E. Aliaga, T. Aguayo, C. Garrido, E. Clavijo, E. Hevia, J. S. Gómez-Jeria, P. Leyton, M. M. Campos-Vallette, S. Sanchez-Cortes, *Biopolymers* **2011**, *95*, 135.
[41] W. Koch, B. Frey, J. F. Sánchez, T. Scior, *Z. Naturforsch. A.* **2003**, *58*, 756.
[42] Hypercube Inc.: 1115 NW 4th Street, Gainesville, Fl. 32601, USA, **2007**.
[43] M. J. Frisch, G. W. Trucks, H. B. Schlegel, G. E. Scuseria, M. A. Robb, J. R. Cheeseman, G. Scalmani, V. Barone, B. Mennucci, G. A. Petersson, H. Nakatsuji, M. Caricato, X. Li, H. P. Hratchian, A. F. Izmaylov, J. Bloino, G. Zheng, J. L. Sonnenberg, M. Hada, M. Ehara, K. Toyota, R. Fukuda, J. Hasegawa, M. Ishida, T. Nakajima, Y. Honda, O. Kitao, H. Nakai, T. Vreven, J. A. Montgomery, Jr., J. E. Peralta, F. Ogliaro, M. Bearpark, J. J. Heyd, E. Brothers, K.N. Kudin, V. N. Staroverov, R. Kobayashi, J. Normand, K. Raghavachari, A. Rendell, J. C. Burant, S. S. Iyengar, J. Tomasi, M. Cossi, N. Rega, J. M. Millam, M. Klene, J. E. Knox, J. B. Cross, V. Bakken, C. Adamo, J. Jaramillo, R. Gomperts, R. E. Stratmann, O. Yazyev, A. J. Austin, R. Cammi, C. Pomelli, J. W. Ochterski, R. L. Martin, K. Morokuma, V. G. Zakrzewski, G. A. Voth, P. Salvador, J. J. Dannenberg, S. Dapprich, A. D. Daniels, O. Farkas, J. B. Foresman, J. V. Ortiz, J. Cioslowski, D.J. Fox, Gaussian 09, Revision A.01, Gaussian, Inc., Wallingford CT, **2009**.
[44] C. Garrido, A. Aliaga, J. S. Gómez-Jeria, J. J. Cárcamo, E. Clavijo, M. M. Campos-Vallette, *Vib. Spectrosc.* **2012**, *61*, 94.
[45] M. S. Kim, S. I. Seok, B. Y. Ahn, S. M. Koo, S. U. Paik, J. Sol-gel, *Science and Technology.* **2003**, *27*, 355.
[46] N. C. Scherrer, S. Zumbuehl, F. Delavy, A. Fritsch, R. Kuehnen, *Spectrochim. Acta A* **2009**, *73*, 505.
[47] W. Herbst, K. Hunger, *Industrial Organic Pigments: Production, Properties, Applications*, 3rd ed., Wiley, Weinheim, **2006**.
[48] D. Lin-Vien, N. B. Colthup, W. G. Fateley, J. G. Graselli, *The Handbook of Infrared and Raman Characteristic Frequencies of Organic Molecules*, 1st ed., Academic Press, Boston, **1991**.
[49] M. R. Marcelino, V. S. F. Muralha, *J. Raman Spectrosc.* **2012**, *43*, 1281.
[50] A. Colombini, D. Kaifas, *e-Preservation Sci.* **2010**, *7*, 14.
[51] S. Q. Lomax, J. F. Lomax, A. De Luca-Westrate, *J. Raman Spectrosc.* **2014**, 45, 448.
[52] 25857 United States Patent Office, 3,109,842. Patented Nov. 5, **1963**.
[53] A. Suwaiyan, R. Zwaricht, N. Baig, *J. Raman Spectrosc.* **1990**, *21*, 243.
[54] V. Krishnakumar, S. Muthunatesan, *Spectrochim. Acta A* **2007**, *66*, 1082.

[55] A. E. Aliaga, C. Garrido, P. Leyton, G. F. Diaz, J. S. Gomez-Jeria, T. Aguayo, E. Clavijo, M. M. Campos-Vallette, S. Sanchez-Cortes, *Spectrochim. Acta A* **2010**, *76*, 458.
[56] R. Aroca, *Surface-Enhanced Vibrational Spectroscopy*, John Wiley & Sons, Chichester, **2006**.

Supporting information

Additional Supporting Information may be found online in the supporting information tab for this article.